Article

Electro-oxidative amination of benzylic C(sp³)–C(sp³) bonds in aromatic hydrocarbons

Kai-Xuan Yang[1], Shu-Fan He[1], Qinhui Wan[1], Tianyi Xu[1], Daixi Li [2,3] ✉, Kexin Liu[4], Wenying Ai[4] ✉ & Tao Shen [1] ✉

C(sp³)-C(sp³) amination represents a promising approach for synthesizing various amines, facilitating applications from late-stage scaffold hopping to the degradation of polymers and biomass. However, it remains challenging due to the inertness of the C-C bond and difficulties in controlling regio- and chemo-selectivity. Herein, we report an electro-oxidative benzylic C(sp³)-C(sp³) amination reaction of aromatic hydrocarbons using nitriles, amides, and sulfonamides as nucleophiles. This process occurs under mild conditions with hydrogen evolution, eliminating the need for external oxidants or transition metal catalysts. Mechanism involves successive anodic oxidative cleavage of the benzylic C(sp³)-C(sp³) bond to generate two carbocation fragments, which are subsequently captured by nucleophiles to form two C-N bonds. Mechanistic studies suggest that HFIP is critical as additive in adjusting the oxidation potentials of alkylbenzene substrates and amine products, effectively preventing overoxidation of products.

Aliphatic C−H and C−C bonds are most fundamental chemical bonds that are widely present in organic compounds[1,2]. Direct functionalization of these inert aliphatic bonds represents a cornerstone in modern organicchemistry. In particular, the functionalization of benzylic C(sp³)−H bonds to construct new carbon-carbon and carbon-heteroatom bonds has been extensively studied[3]. In contrast, the functionalization of ubiquitous benzylic C(sp³)−C(sp³) bonds has been much less explored[4], despite their prevalence and significant potential for enabling late-stage scaffold hopping and facilitating the degradation of persistent polymers and biomass (Fig. 1a). To date, several primary strategies have been developed for C(sp³)−C(sp³) bond cleavage. The first involves ring strain-releasing in a strained system via oxidative addition of low-valent transition metals into C(sp³)−C(sp³) bond[5,6], or single-electron transfer (SET) processes to generate cationic or anionic radicals that drive C(sp³)−C(sp³) bond cleavage and enable difunctionalization[7–15]. Another strategy relies on SET or

hydrogen atom transfer (HAT)-mediated activation of redox-active groups, generating transient oxygen or nitrogen radicals that undergo rapid β-scission[16–21]. Nevertheless, employing such strategies to cleave and functionalize C(sp³)−C(sp³) bonds in acyclic, ubiquitous aromatic hydrocarbons, such as ethane derivatives, still remains a challenging and highly desirable goal due to inherent thermodynamic stability of C(sp³)−C(sp³) bond and low polarization of such substrates. An early example by Alnibi's group demonstrated C(sp³)−C(sp³) bond cleavage of multi-aryl ethanes via arene radical cation intermediates to form C-O bond under photooxidation conditions[22]. Recently, Huang and Chen's group described the elegant photooxidative cleavage of acyclic C(sp³)−C(sp³) bonds in aromatic hydrocarbons to form new C−C bond[23]. More recently, Yu's group made significant breakthroughs in the electro-reductive carboxylation of acyclic C(sp³)−C(sp³) bonds in aromatic hydrocarbons with CO_2, enabling reductive C−C bond cleavage through radical anion intervention[24]. These advancements have

[1]Frontiers Science Center for Transformative Molecules (FSCTM), Shanghai Key Laboratory for Molecular Engineering of Chiral Drugs, School of Chemistry and Chemical Engineering, Zhangjiang Institute for Advanced Study, Shanghai Jiao Tong University, Shanghai, China. [2]Department of Respiratory and Critical Care Medicine, Zhongshan Hospital of Xiamen University, School of Medicine, Xiamen University, Xiamen, China. [3]The School of Clinical Medicine, Fujian Medical University, Fuzhou, China. [4]School of Materials Electronics and Energy Storage, Zhongyuan University of Technology, Zhengzhou, Henan, China. ✉e-mail: lidaixi@xmu.edu.cn; 6786@zut.edu.cn; taoshen@sjtu.edu.cn
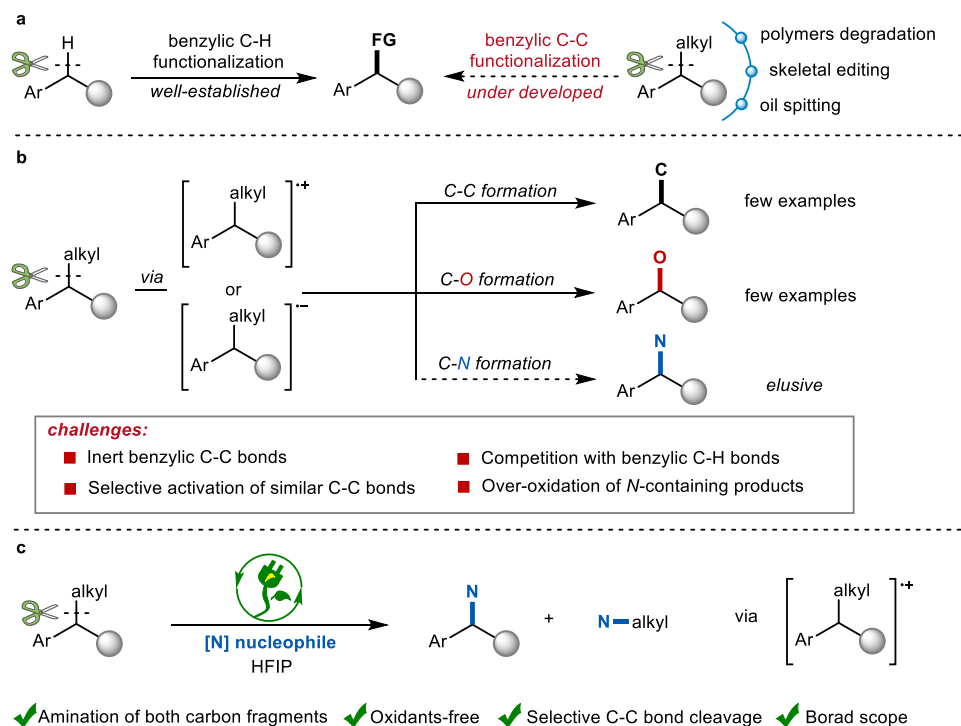
Fig. 1 | Recent advances in benzylic C–C bond functionalization.
a Functionalization of benzylic C–H/C–C bonds. **b** Recent functionalization of benzylic C–C bonds in aromatic hydrocarbons. **c** This work: Electro-oxidative amination of benzylic C–C bonds in aromatic hydrocarbons via HFIP-mediated oxidation potential sorting. HFIP 1, 1, 1, 3, 3, 3-hexafluoro−2-propanol.

significantly expanded the toolbox for C–C and C–O bond formation. Despite this progress, the direct benzylic (sp^3)–C(sp^3) amination in aromatic hydrocarbons to form C–N bonds remains elusive for several challenges (Fig. 1b). Firstly, benzylic C(sp^3)–C(sp^3) bonds are among the most abundant yet the most difficult to cleavage. Secondly, achieving high selectivity is complicated by the coexistence of similar surrounding C–H and C–C bonds. Finally, the risk of overoxidation presents a major challenge in C–C amination chemistry, particularly when the introduced nitrogen lacks sufficient deactivation (e.g., through tosyl protection). Addressing these challenges would open new avenues in C–N bond-forming methodologies and significantly expand the scope of amination chemistry.

Recently, electrochemical[25–43] amination of benzylic C(sp^3)–H have been established[44–53], providing green approaches for C–N bond formation. For example, Xu's group developed a site-selective electrochemical amination reaction that efficiently converts benzylic C–H bonds into C–N linkages[52]. Lambert's group described a method for benzylic C–H bond amination via an electrophotocatalytic Ritter-type reaction[53]. In both cases, the electrochemical single-electron oxidation of the arene substrate to generate an arene radical cation was identified as the key initial step. Building on these previous reports, and given the prevalence and biological significance of amines, we hypothesized that an electro-oxidative method could be developed to induce the amination of widely available benzylic C–C bonds via arene radical cation induced C–C bond cleavage. Herein, we report an electro-oxidative amination of benzylic C(sp^3)–C(sp^3) bonds in aromatic hydrocarbons via HFIP-mediated oxidation potential sorting (Fig. 1c). Notable features of this strategy include: (a) amination of both carbon fragments, dual C–N bond formation from a single C–C cleavage with 200% atom utilization, both resulting carbocationic fragments are efficiently captured via nucleophilic amination, maximizing molecular efficiency and avoiding wasteful byproducts; (b) oxidants free, with hydrogen evolution as the byproduct; (c) highly selective cleavage of benzylic C(sp^3)–C(sp^3) bonds; (d) broad substrate scope,
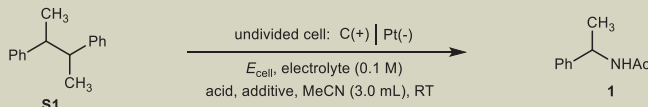
robustness, air tolerance, insensitivity to water, large-scale synthesis; and (e) highly valuable products were formed.

Results and discussion
Reaction development
Initially, butane-2,3-diyldibenzene (**S1**) was selected as the model substrate, and various reaction conditions were tested under a constant voltage for the electro-oxidative amination of benzylic C–C bonds. After thorough optimization, the Ritter-type amination product **1** was obtained in 26% ^{1}H NMR yield under constant voltage (2.4 V) in MeCN, using Et$_4$NBF$_4$ as the supporting electrolyte, carbon cloth as the anode, and a Pt plate as the cathode (Table 1, entry 1). Several electrolytes were tested (entries 2 and 3), with LiClO$_4$ and Et$_4$NOTs yielding only trace amounts of product. We attribute this observation to the critical role played by the electrolyte anion in stabilizing key ionic intermediates and modulating the overall reaction environment. Control experiments revealed that the cell voltage played a critical role, as higher voltages (2.6 V and 2.8 V) resulted in lower yields due to overoxidation of the amide product (entries 4 and 5). The presence of an acid was essential for the transformation, as the yield improved to 33% and 53% with HOTf and MsOH, respectively (entries 6 and 7). This enhancement is likely due to the stabilizing effect of the strong acid on the benzylic cation intermediates. Notably, the yield increased to 79% when HFIP was added as an additive (entry 8), possibly due to its ability to prevent product overoxidation. For comparison, the use of other alcohol additives, such as TFE and EtOH, led to a significant decrease in yield (see Table S2). When the reaction time was shortened to 11 h, the yield further increased to 83%, with a total charge consumption of approximately 260 C (entry 9, E_{anode} = 1.8 V vs SCE, 4.36 mA·cm^{-2} current density). A control reaction conducted in the absence of electricity produced no product (entry 10), confirming that the transformation proceeds via electrochemical oxidation rather than aerobic oxidation. Regarding the electrode materials, several commonly used combinations were evaluated (entries 11–13). Stainless

Table 1 | Optimization of reaction conditions with butane-2,3-diyldibenzene[a]

Entry	Electrolyte	E_{cell}	Acid	Additive	Yield (%)
1	Et₄NBF₄	2.4 V	0.5 mL TFA	–	26
2	LiClO₄	2.4 V	0.5 mL TFA	–	6
3	Et₄NOTs	2.4 V	0.5 mL TFA	–	3
4	Et₄NBF₄	2.6 V	0.5 mL TFA	–	18
5	Et₄NBF₄	2.8 V	0.5 mL TFA	–	18
6	Et₄NBF₄	2.4 V	100 µL TfOH	–	33
7	Et₄NBF₄	2.4 V	100 µL MeSO₃H	–	53
8	Et₄NBF₄	2.4 V	100 µL MeSO₃H	1.0 mL HFIP	79
9[b]	**Et₄NBF₄**	**2.4 V**	**100 µL MeSO₃H**	**1.0 mL HFIP**	**83 (80)[c]**
10	Et₄NBF₄	–	100 µL MeSO₃H	1.0 mL HFIP	0
11[d]	Et₄NBF₄	2.4 V	100 µL MeSO₃H	1.0 mL HFIP	47
12[e]	Et₄NBF₄	2.4 V	100 µL MeSO₃H	1.0 mL HFIP	69
13[f]	Et₄NBF₄	2.4 V	100 µL MeSO₃H	1.0 mL HFIP	64
14	Et₄NBF₄	i = 10 mA	100 µL MeSO₃H	1.0 mL HFIP	58
15[g]	Et₄NBF₄	2.4 V	100 µL MeSO₃H	1.0 mL HFIP	71

[a]Reaction conditions: **S1** (0.3 mmol), electrolyte (0.1 M), MeCN (3.0 mL), carbon cloth anode, Pt plate cathode, rt, in an undivided cell with constant voltage for 16 h under air. Yields determined by ¹H NMR analysis using 1,1,2,2-tetrachloroethane as internal standard. [b]11 h. [c]Isolated yield. [d]Ni as cathode. [e]Stainless steel as cathode. [f]GF020 as anode. [g]MeCN (40 eq.), DCM (2 mL) were used as solvent. DCM Dichloromethane, HFIP 1, 1, 1, 3, 3, 3-hexafluoro-2-propanol, TFA trifluoroacetic acid, TfOH trifluoromethanesulfonic acid, Me methyl, Et ethyl, Ac acetyl.

steel (SS) and nickel (Ni) as cathodes gave inferior results, with lower conversions and diminished selectivity, likely due to inefficient electron transfer and/or competing surface reactions. Among carbon-based anodes, carbon cloth consistently outperformed carbon felt (GF020), affording higher yields under otherwise identical conditions. The relatively poor performance of carbon felt may stem from its higher surface resistance and less uniform current distribution, which can impair reaction efficiency. In addition, conducting the reaction under constant current (10 mA, 6.6 mA/cm² current density) condition resulted in lower yields (entry 14), potentially due to uncontrolled fluctuations in electrode potential that promote undesired oxidative side processes. Finally, we demonstrated that MeCN could function as a reagent (40 equiv.) rather than the reaction solvent, although this modification led to a slight decrease in yield (entry 15). See Table S1 and Table S2 for further details on condition optimization.

Substrate scope evaluation

After establishing the optimized reaction conditions, we proceeded to investigate the scope and general applicability of the reaction, as illustrated in Fig. 2. Initially, symmetric butane-2,3-diyldibenzene substrates were tested. Both butane-2,3-diyldibenzene and 4,4'-dihalogenated butane-2,3-diyldibenzene gave rise to the corresponding benzylacetamides (**1**–**4**) in good yields. A range of butane-2,3-diyldibenzene derivatives with various electron-withdrawing substituents on the benzene rings were also found to be suitable, yielding the corresponding amination products in moderate yields (**2**–**6, 12**–**17**). Notably, the aldehyde functional group, despite its well-known sensitivity to oxidative conditions, was well tolerated under our electrochemical protocol (**14**), although a significant amount of starting material was recovered, likely due to its limited reactivity under the current conditions. When examining substrates designed to probe the competition between benzylic C–H and benzylic C–C bonds, we observed that the C–C amination products (**7, 8,** and **11**) were preferentially formed, rather than the alternative benzylic methyl or ethyl-functionalized sites. However, the linear para-*n*-butyl

substrate afforded product **10** in 29% yield, along with 9% competing C–H amination byproduct. Notably, no benzylic C–H amination products were observed at the same benzylic position in branched substrates where C–C bond amination occurred. This strongly supports our hypothesis that C–C cleavage is the kinetically and thermodynamically favored pathway at the benzylic position under the reaction conditions. The main reason for the moderate yields observed with electron-rich substrates is product overoxidation and decomposition. In addition, the competitive formation of ketone side products via C–C bond oxidation (for **9**, 40% yield of ketone formed), promoted by trace amounts of water in the system, also contributes to the reduced efficiency (See Section 2.6 'Side product analysis' in the Supplementary Information.). We propose that for electron-rich substrates, the high reactivity facilitates rapid C–C bond cleavage, generating highly reactive radical or carbocation intermediates. While these intermediates can undergo competitive side reactions with trace amounts of water present in the system, resulting in the formation of ketone byproducts. For a substrate bearing more electron-donating methoxy groups **S18** underwent selective amination to provide the corresponding products in 62% yields (**18**). The influence of alkyl chain length was also assessed, and all substrates proceeded smoothly under the standard conditions, producing the corresponding amination products in moderate to good yields (**19** to **26**). For asymmetric substrates with different substituents on the benzene ring or various alkyl groups, two distinct benzylic amination products were obtained (**27**–**29, 31**). Unfortunately, the thiophene-substituted amide (**30**) was not observed due to the degradation of the desired product, as well as substrates bearing a furan moiety (see Fig. S7), likely caused by the low oxidative potential of the thiophene and furan groups. Similarly, substrate **31** underwent smooth carbon-carbon bond cleavage to afford the ketone **32** in 27% yield instead of C–C amination product, suggesting that the electron-rich nature of thiophene may render the intermediate species more susceptible to overoxidation. Finally, the average Faradaic efficiency under the optimized conditions is
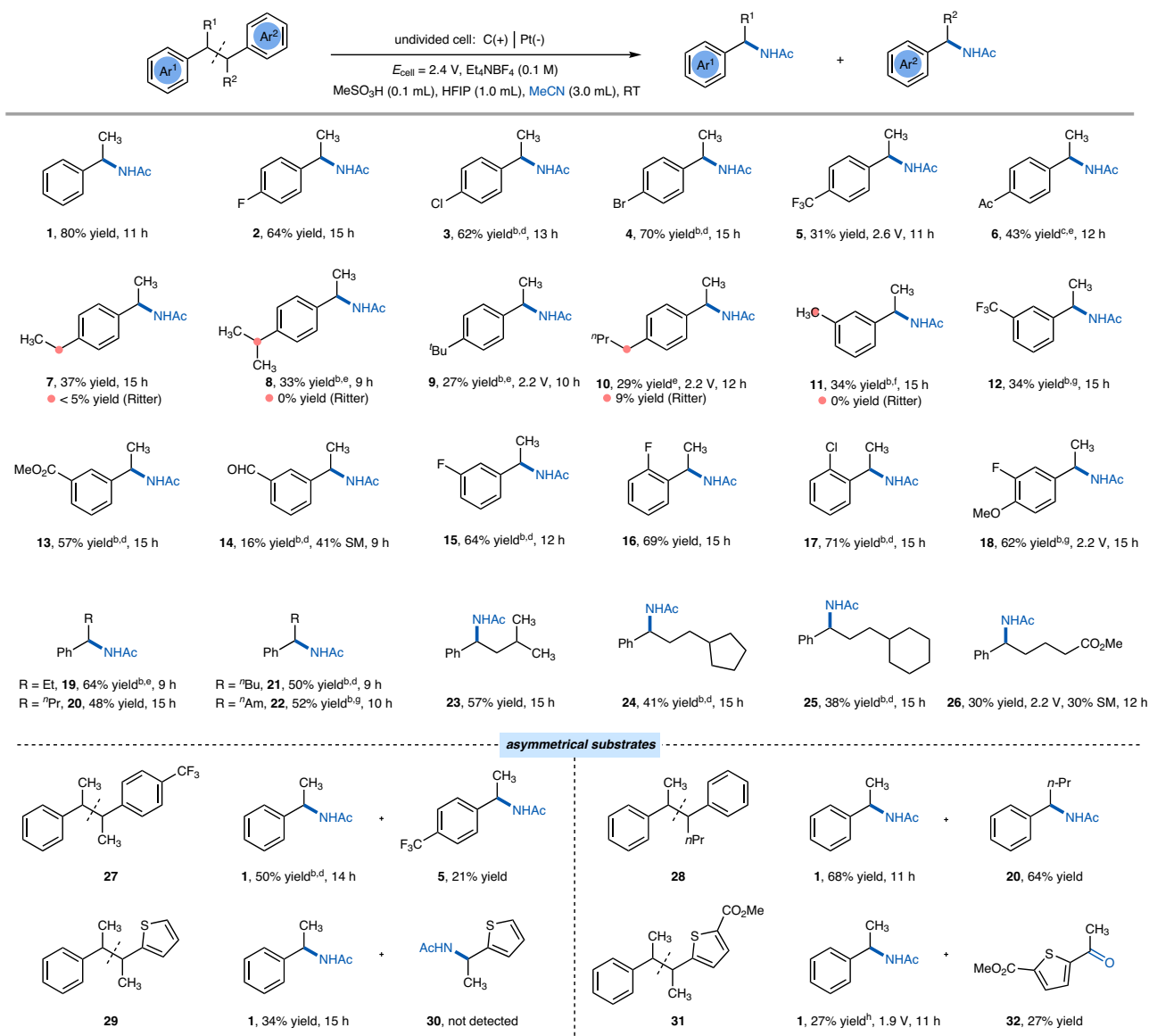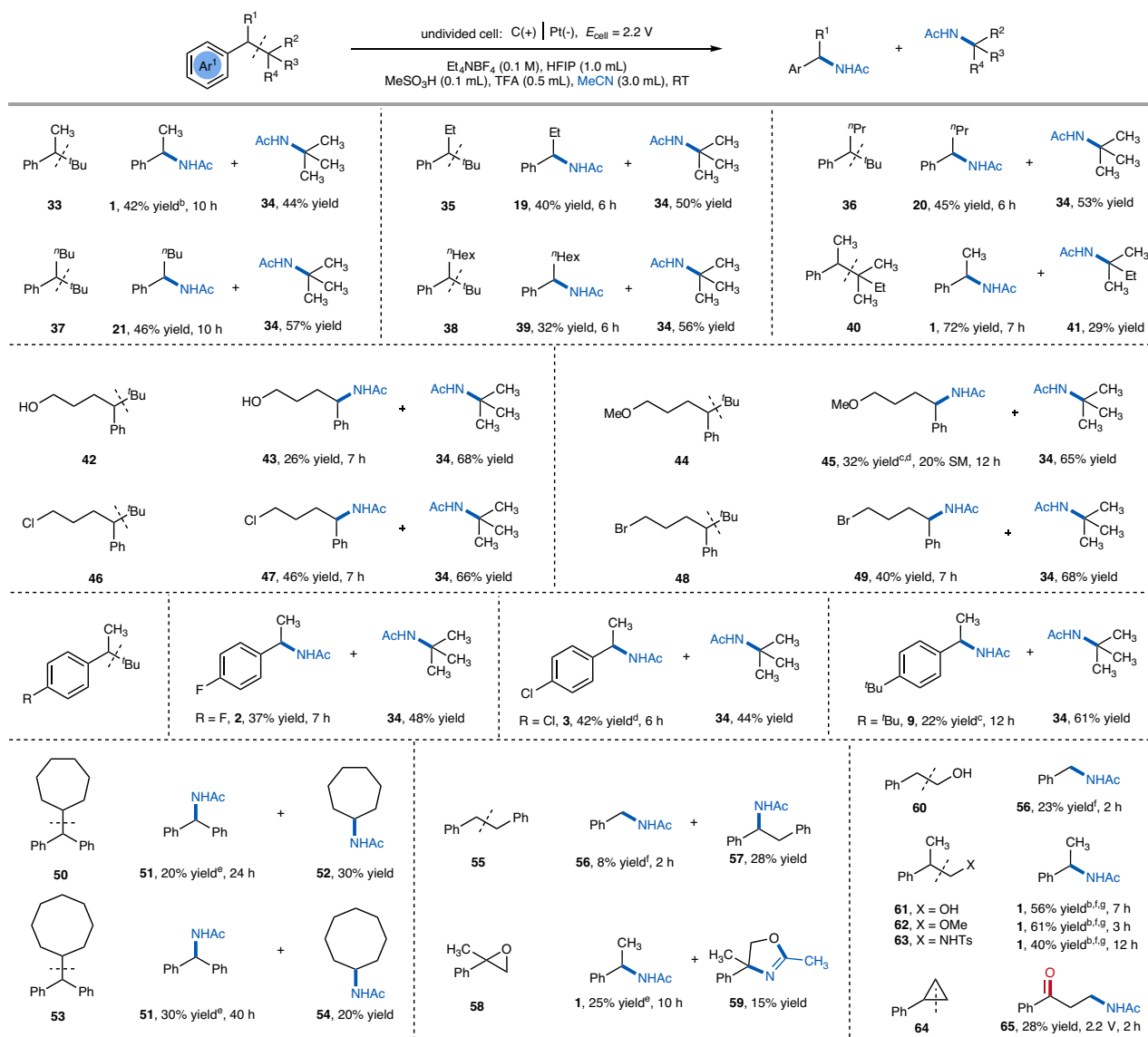
Fig. 2 | Scope of electrooxidative C–C bond amination of bisbenzylic substrates[a]. [a]Reaction conditions: substrates (0.3 mmol), Et$_4$NBF$_4$ (0.1 M), MeCN (3.0 mL), HFIP (1.0 mL), MeSO$_3$H (0.1 mL), carbon cloth anode, Pt plate cathode, rt, in an undivided cell with constant voltage (2.4 V), under air atmosphere. Isolated yields are calculated based on a theoretical maximum of 200% based on the fact that the starting material contains two equivalents. [b]Et$_4$NBF$_4$ (0.2 M), graphite felt anode. [c]Graphite felt anode. [d]MeSO$_3$H (0.15 mL), TFA (0.6 mL). [e]MeSO$_3$H (0.1 mL),

TFA (0.6 mL). [f]MeSO$_3$H (0.15 mL). [g]MeSO$_3$H (0.10 mL) for 10 h, an extra MeSO$_3$H (0.10 mL) was added for another 5 h. [h]0.1 mmol scale. Unsuccessful examples are provided in the Supplementary Information. The total consumed charge and Far-adaic efficiency for representative substrates were included in the Supplementary information. HFIP 1, 1, 1, 3, 3, 3-hexafluoro-2-propanol, TFA trifluoroacetic acid, Me methyl, Et ethyl, Ac acetyl, ^{t}Bu tert-butyl, ^{n}Bu n-butyl, ^{n}Pr n-propyl, ^{n}Am n-amyl.

approximately 30%, calculated based on the total charge passed and the amount of product formed (see Fig. S9).

In addition to dibenzyl-substituted substrates, inert, unactivated substrates with bulky alkyl groups can also successfully yield two target products (Fig. 3). Such bulky groups can decrease the bond dissociation energy (BDE) of the C–C bond by stabilizing the formed fragments, thus exerting a thermodynamic and steric effect[54–56]. We examined a series of homobenzylic and neopentylic substrates featuring inert, unactivated aliphatic C(sp^3)–C(sp^3) bonds. For instance, α-methyl neopentylbenzene (compound **33**) underwent efficient cleavage and amination, affording two products in moderate yields. Furthermore, various α-branched neopentylbenzenes (compounds **35–38**) bearing chains of differing lengths were well tolerated, consistently affording cleaved and aminated products in moderate to good yields. Importantly, increasing steric bulk (e.g., products **1, 41**)

did not impede the reaction, suggesting that steric hindrance does not critically limit the method's applicability. Notably, the cleavage selectively occurred at the more hindered tertiary center (tert-butyl), while another benzylic C–C bond remained intact, highlighting the excellent regioselectivity of the transformation. In terms of functional group compatibility, our method tolerated a range of oxidatively sensitive groups, including primary alcohols (**43**), methyl ethers (**45**), alkyl chlorides (**47**), and bromides (**49**). These examples further support the mildness and chemoselectivity of the electrochemical conditions. Mildly electron-deficient alkylbenzenes underwent successful oxidation. Notably, neopentylbenzene bearing a para-tert-butyl substituent afforded the aminated product **34** in 61% yield. In contrast, product **9** was obtained in only a 22% yield, likely due to competing oxidative side reactions leading to ketone formation.

Fig. 3 | Scope of electrooxidative C−C bond amination of unactivated alkylbenzenes[a]. [a]Reaction conditions: substrates (0.3 mmol), Et$_4$NBF$_4$ (0.1 M), MeCN (3.0 mL), HFIP (1.0 mL), MeSO$_3$H (0.1 mL), TFA (0.5 mL), graphite felt anode, Pt plate cathode, rt, in an undivided cell with constant voltage (2.2 V), under air atmosphere. Isolated yield. [b]Substrates (0.6 mmol). [c]Constant voltage (2.1 V). [d]Carbon cloth anode. [e]Constant voltage (2.4 V), carbon cloth anode, w/o TFA.

[f]Et$_4$NBF$_4$ (0.2 M), MeSO$_3$H (0.15 mL), TFA (0.5 mL). [g]Constant voltage (2.4 V). The total consumed charge and Faradaic efficiency for representative substrates were included in the Supplementary Information. HFIP 1, 1, 1, 3, 3, 3-hexafluoro-2-propanol, TFA trifluoroacetic acid, Me methyl, Et ethyl, Ac acetyl, [t]Bu tert-butyl, [n]Bu n-butyl, [n]Pr n-propyl, [n]Hex n-hexyl.

Using this strategy, we successfully synthesized cycloheptylacetamide **52** and cyclooctylacetamide **54** (Fig. 3). Due to the stability of the dibenzyl radical, the cleavage of such substrates demonstrates excellent regioselectivity. However, it is important to note that the low yield is attributed to the formation of benzophenone (~20% yield), likely due to trace amounts of water present during the reaction. For unbranched substrate **55**, the benzylic C−H amination was the predominant pathway and only 8% C−C cleavage product was detected. Beyond simple hydrocarbons, substrates containing heteroatom substitutions were also tested under standard conditions. For instance, epoxy-containing substrate **58** underwent C−C bond cleavage to generate amide **1** and C−O bond cleaved product **59**. It is well known that oxygen and nitrogen atom can initiate β−C−C bond cleavage (**61**–**63**) by through-bond delocalization and electron apportionment to the fragments (via cation and radical-stabilizing effects)[16–21]. Under standard reaction conditions, these substrates underwent β−C−C bond cleavage to form the

corresponding amides, although the yield was lower for the unbranched substrate **64**. We hypothesize that the cleavage of these substrates involves two contributions: (1) the formation of nitrogen or oxygen radicals via electrochemical oxidation, leading to β−C−C bond cleavage; and (2) β−C−C cleavage initiated by aryl cation radicals. For comparison, when using 1,2-diphenylethane **55** as a substrate, only an 8% yield was obtained, suggesting that the formation of oxygen radicals may be involved for the cleavage of primary (1°) alcohol substrates. Lastly, strained ring substrate **64** smoothly underwent ring-opening 1, 3-difunctionalization to yield β-amino ketones **65**.

Additionally, further investigation of various nitriles revealed a wide compatibility with Cl (**66, 68**), Br (**67**), Pr (**69**), and Ph (**70**) (Fig. 4). Other suitable nitrogen nucleophiles included methanesulfonamide (**71**), ethanesulfonamide (**72**), oxazolidin-2-one (**73**), and carbamate (**74**). Of particular interest is the functionalization of the benzylic C−C bond with oxygen nucleophiles, including acetates (**75**–**80**). Notably, a
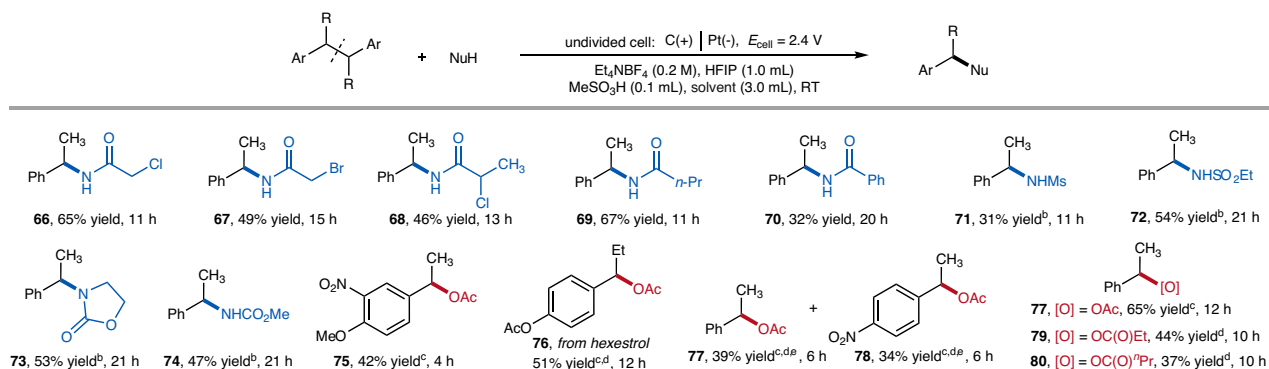
Fig. 4 | Scope of nucleophiles[a]. [a]Reaction conditions: For **66**–**70** and **75**–**80**: S1 (0.3 mmol), Et$_4$NBF$_4$ (0.2 M), corresponding nitrile solvent (3 mL) or acid solvent (3 mL), HFIP (1.0 mL), MeSO$_3$H (0.1 mL), graphite felt (2 mm) anode, Pt cathode at rt, in an undivided cell with constant voltage (2.4 V), under air atmosphere. Isolated yield. [b]Reactions performed with 3.6 mmol nucleophile (**71**: MsNH$_2$, **72**: EtSO$_2$NH$_2$,

73: 2-oxazolidone, **74**: urethane) in 3 mL DCM. [c]0.8 mL TFA was used. [d]Graphite felt (6.5 mm) was used as anode. [e]0.1 mmol of substrate. HFIP 1, 1, 1, 3, 3, 3-hexafluoro-2-propanol, TFA trifluoroacetic acid, DCM dichloromethane, Ac acetyl, Ms methanesulfonyl, [n]Pr n-propyl.
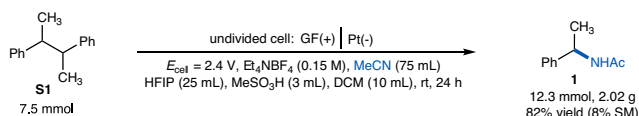
Fig. 5 | Gram scale synthesis of 1. HFIP 1, 1, 1, 3, 3, 3-hexafluoro-2-propanol, DCM dichloromethane, Me methyl, Ac acetyl.

strong electron-withdrawing group, nitro, proved compatible, affording products **78** in 34% yields.

The electrochemical C–C amination reaction was successfully carried out on a gram scale, as illustrated by the synthesis of **1** (Fig. 5), where larger electrodes were used over an extended reaction time. Note that DCM was added as a co-solvent to improve the solubility of the starting material thereby ensuring a homogeneous reaction mixture and maintaining efficient mass and electron transfer throughout the electrolysis process.

Mechanistic investigations

Several mechanistic experiments were carried out to gain insight into the mechanism. Firstly, control experiments were performed to investigate the influence of water and oxygen in the air on the reaction. Under a strictly nitrogen atmosphere, the reaction yield remained stable at around 80%, while no significant promotional effect was observed under oxygen conditions, suggesting that the reaction likely does not involve dioxygen-induced C–C bond cleavage. Furthermore, the impact of varying the amount of water additive was carefully examined, with equivalents ranging from 0.5 to 2.0. The results showed little effect on the yield, indicating that the presence of water does not significantly promote the formation of the target product (Fig. 6a). Additionally, no benzylic alcohol intermediate was detected during the reaction. Besides, when the synthesized benzylic alcohol substrate **81** was subjected to the standard conditions, no product was formed. On the contrary, the substrate almost completely degraded under these conditions (Fig. 6b). These experiments suggest that benzylic tertiary (3°) alcohol is likely not a key intermediate in the reaction, despite numerous reports on C–C bond cleavage initiated by benzylic alcohol-derived oxygen radicals[16–21].

Furthermore, the electrode voltage was continuously recorded throughout the electrolysis of the model reaction. Anodic oxidation was maintained at approximately 2.16 V vs. Ag/AgCl (Fig. 6c). These results are consistent with the oxidative potential of substrates. Furthermore, cyclic voltammograms of butane-2,3-diyldibenzene (**S1**) and it's aminated product (**1**) were recorded in MeCN (Fig. 6d). The results
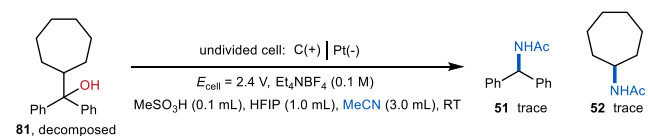
revealed that butane-2,3-diyldibenzene ($E_{p/2}$ = 2.30 V vs SCE) was oxidized at higher potential than product **1** ($E_{p/2}$ = 2.15 V vs SCE), indicating that the aminated product exhibits a greater tendency for overoxidation in MeCN. In contrast, cyclic voltammograms of **S1** and **1** in a MeCN/HFIP (3/1) solvent mixture showed that butane-2,3-diyldibenzene ($E_{p/2}$ = 1.97 V vs SCE) was oxidized at a bit lower potential than product **1** ($E_{p/2}$ = 2.00 V vs SCE) (Fig. 6d). Although the oxidation potentials of butane-2,3-diyldibenzene (**S1**) and product (**1**) differ only slightly, they were effectively distinguished during the preparative electrolysis performed in MeCN/HFIP. The significance of HFIP lies in its ability to stabilize radical cation intermediates, facilitating substrate oxidation while preventing overoxidation of the product[52].

Based on these experiments, a plausible mechanism was proposed (Fig. 6e). During the anode phase, single-electron oxidation of the aromatic hydrocarbons **A** generates the radical cation **B**, which undergoes homolytic β-C–C bond cleavage to form a benzylic cation **C** and a radical species **E** at another position or heterolytic mode of cleavage to generate benzylic radical **C'** and species **E'**, depending on the relative oxidation potentials of the two fragments formed[23,57,58]. For example, heterolytic cleavage to generate [t]Bu cation is preferred due to the lower oxidation potential of [t]Bu radical (Eox 1/2([t]Bu·) = 0.41 V vs SCE, Eox 1/2(MeCH$_2$Ph) = 0.82 V vs SCE, $\Delta\Delta G$ = −23.06 × (0.82−0.41) = −9.5 kcal/mol)[59]. The process may be reversible, and due to the small intrinsic barrier (0.1–0.2 eV), fragment diffusion from the solvent cage could be the rate-limiting step in endergonic cleavages[60,61]. The lower intrinsic barrier for C–C bond cleavage compared to deprotonation may account for the observation that C–C bond cleavage effectively competes with C–H bond cleavage. It is worth noting that the oxidation potentials of the generated benzyl and alkyl radical intermediates are typically below 1.0 V vs SCE[57]. As a result, under the present electrooxidation conditions (E_{anode} = 2.1 V vs Ag/AgCl), their lifetimes are extremely short, making them difficult to capture and prone to direct oxidation at the anode. Regardless of β-C–C bond cleavage model, above radical intermediates **C'** and **E** undergoes a second, rapid oxidation event directly at the anode, resulting in the formation of final carbocations **C** and **E'**. Both carbocations subsequently proceed through the classic Ritter reaction steps to yield the amide product **D** and **F**. When nucleophiles such as sulfonamides, amides, or carboxylic acids were employed, the corresponding cross-coupling products were formed. Meanwhile, the redox reaction is balanced by cathodic proton reduction, leading to the production of hydrogen. Notably, due to the extensive use of bulky alkyl substituents and biaryl substrates in this work, in most cases, benzylic C(sp^3)–C(sp^3) cleavage competes effectively with C–H bond cleavage. Thus, the formation of
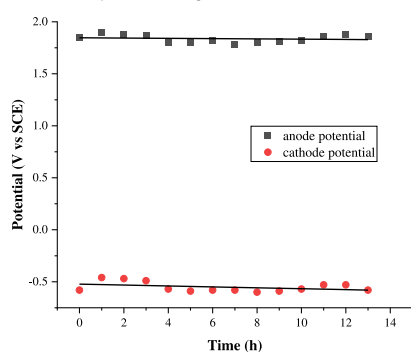
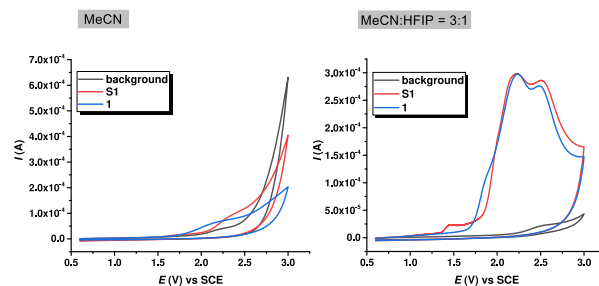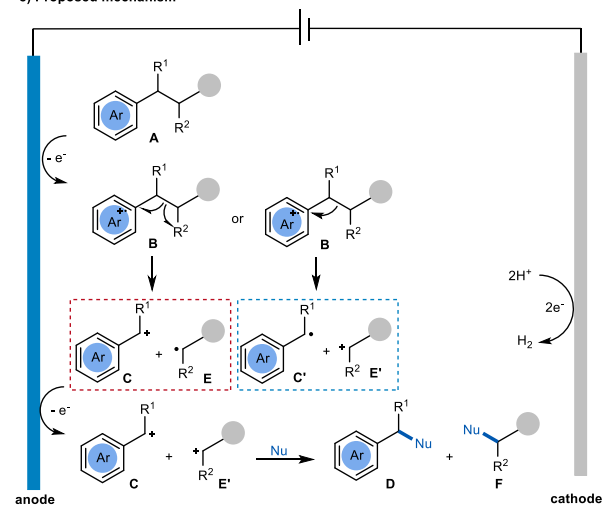**Fig. 6 | Mechanistic studies and proposal. a** Control reaction with **S1**. **b** Control reaction with benzylic alcohol. **c** Anode and cathode potential during the reaction. **d** Investigation of the role of HFIP. **e** Proposed mechanism. HFIP 1, 1, 1, 3, 3, 3-hexafluoro-2-propanol, Me methyl, Ac acetyl, Nu Nucleophile.

benzyl tertiary (3°) alcohols or benzyl hydroperoxide species is unfavorable under these conditions.

In summary, we have developed an electro-oxidative benzylic C(sp³)–C(sp³) amination reaction that operates under mild conditions with H₂ evolution, eliminating the need for external oxidants or transition metal catalysts. This method is not only suitable for the efficient and scalable synthesis of benzylic amines but also demonstrates excellent compatibility with various nucleophiles, demonstrating significant potential for advancing sustainable C–C functionalization reactions using simple materials.

Methods
General procedure for acetamidation product
An oven-dried, undivided three-necked cell (20 mL) equipped with a magnetic stir bar, carbon cloth anode (15 mm × 15 mm × 0.3 mm) and Pt plate cathode (15 mm × 15 mm × 0.3 mm). To the cell was added Et₄NBF₄ (95.9 mg, 0.41 mmol, 0.1 M), MeCN (3 mL), HFIP (1 mL) and butane-2,3-diyldibenzene (63.0 mg, 0.3 mmol). The mixture was stirred for 1 min, and then MsOH (0.1 mL) was carefully added. The solution was then stirred at room temperature and electrolysis was initiated at a control voltage of 2.4 V for the specified amount of time. After completion of the reaction as monitored by TLC (usually 8–18 h), the reaction mixture was poured into a saturated sodium carbonate solution (ca. 20 mL). The carbon cloth anode was washed with EtOAc (3 × 10 mL) and these washes were added to the reaction mixture. The aqueous layer was separated and extracted with EtOAc (3 × 15 mL), and the combined organic layers were washed with brine and dried over anhydrous Na₂SO₄. Following concentration in vacuo, the crude product was purified by preparative thin-layer chromatography (PTLC) (eluent: petroleum ether: ethyl acetate = 2:1 to 1:1) to afford pure product.

General procedure for other amine nucleophilic reagents product
An oven-dried undivided three-necked cell (20 mL) equipped with a magnetic stir bar, graphite felt anode (15 mm × 15 mm × 2 mm) and Pt plate cathode (15 mm × 15 mm × 0.3 mm). To the cell was added Et₄NBF₄ (204 mg, 0.94 mmol, 0.2 M), DCM (3 mL), HFIP (1 mL), nucleophiles (3.6 mmol) and butane-2,3-diyldibenzene (63.0 mg, 0.3 mmol). The mixture was stirred for 1 min, and then MsOH (0.10 mL), TFA (0.6 mL) was carefully added. The solution was then stirred at room temperature under and electrolysis was initiated at a control voltage of 2.4 V for the specified amount of time. After completion of the reaction as monitored by TLC (usually 8–20 h), the reaction mixture was poured into a saturated sodium carbonate solution (ca. 20 mL). The carbon cloth anode was washed with EtOAc (3 × 10 mL), and these washes were added to the reaction mixture. The aqueous layer was separated and extracted with EtOAc (3 × 15 mL), and the combined organic layers were washed with brine and dried over anhydrous Na₂SO₄. Following concentration in vacuo, the crude product was purified by preparative thin-layer chromatography (PTLC) (eluent: petroleum ether: ethyl acetate = 5:1 to 1:1) to afford pure product.

Data availability
The data generated in this study are provided in the Supplementary Information, All data are available from the corresponding author upon request.

References

1. Trost, B. M. & Fleming, I. Comprehensive organic synthesis: selectivity, strategy, and efficiency in modern organic chemistry. **8**, (Elsevier, 1991).
2. Ritleng, V., Sirlin, C. & Pfeffer, M. Ru-, Rh-, and Pd-catalyzed C–C bond formation involving C–H activation and addition on unsaturated substrates: reactions and mechanistic aspects. *Chem. Rev.* **102**, 1731–1770 (2002).
3. Lam, N. Y. S., Wu, K. & Yu, J.-Q. Advancing the logic of chemical synthesis: C–H activation as strategic and tactical disconnections for C–C bond construction. *Angew. Chem. Int. Ed.* **60**, 15767–15790 (2021).
4. Drahl, M. A., Manpadi, M. & Williams, L. J. C–C fragmentation: origins and recent applications. *Angew. Chem. Int. Ed.* **52**, 11222–11251 (2013).
5. Souillart, L. & Cramer, N. Catalytic C–C bond activations via oxidative addition to transition metals. *Chem. Rev.* **115**, 9410–9464 (2015).
6. Murakami, M. & Ishida, N. Potential of metal-catalyzed C–C single bond cleavage for organic synthesis. *J. Am. Chem. Soc.* **138**, 13759–13769 (2016).
7. Huang, W., Keess, S. & Molander, G. A. Dicarbofunctionalization of [1.1.1] propellane enabled by nickel/photoredox dual catalysis: one-step multicomponent strategy for the synthesis of BCP-aryl derivatives. *J. Am. Chem. Soc.* **144**, 12961–12969 (2022).
8. Frank, N. et al. Synthesis of meta-substituted arene bioisosteres from [3.1.1] propellane. *Nature* **611**, 721–726 (2022).
9. Ociepa, M., Wierzba, A. J., Turkowska, J. & Gryko, D. Polarity-reversal strategy for the functionalization of electrophilic strained molecules via light-driven cobalt catalysis. *J. Am. Chem. Soc.* **142**, 5355–5361 (2020).
10. Zheng, Y. et al. Photochemical intermolecular [3σ+2σ]-cycloaddition for the construction of aminobicyclo [3.1.1] heptanes. *J. Am. Chem. Soc.* **144**, 23685–23690 (2022).
11. Ge, L. et al. Photoredox-catalyzed C–C bond cleavage of cyclopropanes for the formation of C(sp^3)-heteroatom bonds. *Nat. Commun.* **13**, 5938 (2022).
12. Kolb, S. et al. Electrocatalytic activation of donor-acceptor cyclopropanes and cyclobutanes: an alternative C(sp^3)–C(sp^3) cleavage mode. *Angew. Chem. Int. Ed.* **60**, 15928–15934 (2021).
13. Peng, P. et al. Electrochemical C–C bond cleavage of cyclopropanes towards the synthesis of 1, 3-difunctionalized molecules. *Nat. Commun.* **12**, 3075 (2021).
14. Liao, L.-L. et al. Electrochemical ring-opening dicarboxylation of strained carbon-carbon single bonds with CO_2: facile synthesis of diacids and derivatization into polyesters. *J. Am. Chem. Soc.* **144**, 2062–2068 (2022).
15. Liu, Y. et al. Photocatalytic dicarboxylation of strained C–C bonds with CO_2 via consecutive visible-light-induced electron transfer. *Chin. Chem. Lett.* **35**, 109138–109143 (2024).
16. Yu, X.-Y., Chen, J.-R. & Xiao, W.-J. Visible light-driven radical-mediated C–C bond cleavage/functionalization in organic synthesis. *Chem. Rev.* **121**, 506–561 (2020).
17. Morcillo, S. P. Radical-promoted C–C bond cleavage: a deconstructive approach for selective functionalization. *Angew. Chem. Int. Ed.* **58**, 14044–14054 (2019).
18. Wu, X. & Zhu, C. Recent advances in alkoxy radical-promoted C–C and C–H bond functionalization starting from free alcohols. *Chem. Commun.* **55**, 9747–9756 (2019).
19. Tsui, E., Wang, H. & Knowles, R. R. Catalytic generation of alkoxy radicals from unfunctionalized alcohols. *Chem. Sci.* **11**, 11124–11141 (2020).
20. Wang, Y. et al. Visible-light-promoted site-specific and diverse functionalization of a C(sp^3)–C(sp^3) bond adjacent to an arene. *ACS Catal.* **10**, 6603–6612 (2020).
21. Vanderghinste, J. & Das, S. Applications of photoredox catalysis for the radical-induced cleavage of C–C Bonds. *Synthesis* **54**, 3383–3398 (2022).
22. Albini, A., Fasani, E. & Mella, M. Photochemical reaction of 1, 4-naphthalenedicarbonitrile with alkylbenzenes and bibenzyls. *J. Am. Chem. Soc.* **108**, 4119–4125 (1986).
23. Liao, K. et al. Photoredox cleavage of a Csp^3–Csp^3 bond in aromatic hydrocarbons. *J. Am. Chem. Soc.* **145**, 12284–12292 (2023).
24. Ran, C.-K. et al. Electro-reductive carboxylation of acyclic C(sp^3)–C(sp^3) bonds in aromatic hydrocarbons with CO_2. *Sci. China Chem.* **67**, 3366–3372 (2024).
25. Francke, R. & Little, R. D. Redox catalysis in organic electrosynthesis: basic principles and recent developments. *Chem. Soc. Rev.* **43**, 2492–2521 (2014).
26. Yan, M., Kawamata, Y. & Baran, P. S. Synthetic organic electrochemical methods since 2000: on the verge of a renaissance. *Chem. Rev.* **117**, 13230–13319 (2017).
27. Wiebe, A. et al. Electrifying organic synthesis. *Angew. Chem. Int. Ed.* **57**, 5594–5619 (2018).
28. Pletcher, D., Green, R. A. & Brown, R. C. D. Flow electrolysis cells for the synthetic organic chemistry laboratory. *Chem. Rev.* **118**, 4573–4591 (2017).
29. Jiang, Y., Xu, K. & Zeng, C. Use of electrochemistry in the synthesis of heterocyclic structures. *Chem. Rev.* **118**, 4485–4540 (2017).
30. Kärkäs, M. D. Electrochemical strategies for C–H functionalization and C–N bond formation. *Chem. Soc. Rev.* **47**, 5786–5865 (2018).
31. Yoshida, J.-I., Shimizu, A. & Hayashi, R. Electrogenerated cationic reactive intermediates: the pool method and further advances. *Chem. Rev.* **118**, 4702–4730 (2018).
32. Xiong, P. & Xu, H.-C. Chemistry with electrochemically generated *N*-centered radicals. *Acc. Chem. Res.* **52**, 3339–3350 (2019).
33. Little, R. D. A perspective on organic electrochemistry. *J. Org. Chem.* **85**, 13375–13390 (2020).
34. Siu, J. C., Fu, N. & Lin, S. Catalyzing electrosynthesis: a homogeneous electrocatalytic approach to reaction discovery. *Acc. Chem. Res.* **53**, 547–560 (2020).
35. Meyer, T. H., Choi, I., Tian, C. & Ackermann, L. Powering the future: how can electrochemistry make a difference in organic synthesis?. *Chem* **6**, 2484–2496 (2020).
36. Jiao, K.-J., Xing, Y.-K., Yang, Q.-L., Qiu, H. & Mei, T.-S. Site-selective C–H functionalization via synergistic use of electrochemistry and transition metal catalysis. *Acc. Chem. Res.* **53**, 300–310 (2020).
37. Novaes, L. F. T. et al. Electrocatalysis as an enabling technology for organic synthesis. *Chem. Soc. Rev.* **50**, 7941–8002 (2021).
38. Yuan, Y., Yang, J. & Lei, A. Recent advances in electrochemical oxidative cross-coupling with hydrogen evolution involving radicals. *Chem. Soc. Rev.* **50**, 10058–10086 (2021).
39. Ma, C. et al. Recent advances in organic electrosynthesis employing transition metal complexes as electrocatalysts. *Sci. Bull.* **66**, 2412–2429 (2021).
40. Cheng, X. et al. Recent applications of homogeneous catalysis in electrochemical organic synthesis. *CCS Chem.* **4**, 1120–1152 (2022).
41. Liu, Y., Li, P., Wang, Y. & Qiu, Y. Electroreductive cross-electrophile coupling (eXEC) reactions. *Angew. Chem. Int. Ed.* **62**, e202306679 (2023).
42. Chang, X., Zhang, Q. & Guo, C. Asymmetric electrochemical transformation. *Angew. Chem. Int. Ed.* **59**, 12612–12622 (2020).
43. Shi, S.-H., Liang, Y. & Jiao, N. Electrochemical oxidation induced selective C–C bond cleavage. *Chem. Rev.* **121**, 485–505 (2021).
44. Meng, Z., Feng, C. & Xu, K. Recent advances in the electrochemical formation of carbon-nitrogen bonds. *Chin. J. Org. Chem.* **41**, 2535–2570 (2021).
45. Liang, Y. et al. Using a nitrogen-centered radical as a selective mediator in electrochemical C(sp^3)-H amination. *Chem. Catal.* **3**, 100582–100593 (2023).

46. Kathiravan, S. & Nicholls, I. A. Recent advances in electrochemical C–N bond formation via C–H/N–H activation with hydrogen evolution. *Curr. Res. Green. Sustain. Chem.* **8**, 100405–100431 (2024).

47. Yu, Y., Zhu, X.-B., Yuan, Y. & Ye, K.-Y. An electrochemical multicomponent reaction toward C–H tetrazolation of alkyl arenes and vicinal azidotetrazolation of alkenes. *Chem. Sci.* **13**, 13851–13856 (2022).

48. Yu, M. et al. Electrochemical-induced benzyl C–H amination towards the synthesis of isoindolinones via aroyloxy radical-mediated C–H activation. *Green. Chem.* **24**, 1445–1450 (2022).

49. Zhang, L. et al. Ritter-type amination of C(sp^3)–H bonds enabled by electrochemistry with SO_4^{2-}. *Nat. Commun.* **13**, 4138 (2022).

50. Hayashi, R. et al. Metal-free benzylic C–H amination via electrochemically generated benzylaminosulfonium ions. *Chem. Eur. J.* **23**, 61–64 (2017).

51. Choi, A. et al. Electrochemical benzylic C(sp^3)–H direct amidation. *Org. Lett.* **26**, 653–657 (2024).

52. Hou, Z.-W. et al. Site-selective electrochemical benzylic C–H amination. *Angew. Chem. Int. Ed.* **60**, 2943–2947 (2021).

53. Shen, T. & Lambert, T. H. C–H amination via electrophotocatalytic Ritter-type reaction. *J. Am. Chem. Soc.* **143**, 8597–8602 (2021).

54. Baciocchi, E., Bietti, M. & Lanzalunga, O. Mechanistic aspects of β-bond-cleavage reactions of aromatic radical cations. *Acc. Chem. Res.* **33**, 243–251 (2000).

55. Popielarz, R. & Arnold, D. R. Radical ions in photochemistry. Part 24. Carbon-carbon bond cleavage of radical cations in solution: theory and application. *J. Am. Chem. Soc.* **112**, 3068–3082 (1990).

56. Arnold, D. R. & Lamont, L. J. Photosensitized (electron transfer) carbon–carbon bond cleavage of radical cations: the 2-phenylethyl ether and acetal systems. *Can. J. Chem.* **67**, 2119–2127 (1989).

57. Wayner, D. D. M., McPhee, D. J. & Griller, D. Oxidation and reduction potentials of transient free radicals. *J. Am. Chem. Soc.* **110**, 132–137 (1988).

58. Maslak, P. Fragmentations by photoinduced electron transfer. Fundamentals and practical aspects. *Top. Curr. Chem.* **168**, 1–46 (1993).

59. Fu, Y., Liu, L., Yu, H.-Z., Wang, Y.-M. & Guo, Q.-X. Quantum chemical predictions of absolute standard redox potentials of diverse organic molecules and free radicals in acetonitrile. *J. Am. Chem. Soc.* **127**, 7227–7234 (2005).

60. Anne, A., Fraoua, S., Moiroux, J. & SaveÂant, J.-M. Thermodynamic control in ion radical cleavages through out-of-cage diffusion of products. Dynamics of C–C fragmentation in cation radicals of tert-butylated NADH analogues and other ion radicals. *J. Am. Chem. Soc.* **118**, 3938–3945 (1996).

61. Maslak, P., Vallombroso, T. M., Chapman, W. H. Jr & Narvaez, J. N. Free-energy relationship for mesolytic cleavage of C–C bonds. *Angew. Chem. Int. Ed.* **3**, 73–75 (1994).

Acknowledgements

Author contributions

T. S. conceived of and directed the project and prepared the manuscript. T. S., D. L., W. A. and K.-X. Y. designed experiments. K.-X. Y., S.-F. H., Q. W., T. X. and K. L. performed the experiments and analyzed the data. All the authors participated in the discussion and preparation of the manuscript.

Competing interests

The authors declare no competing interests.

Additional information

Supplementary information The online version contains supplementary material available at https://doi.org/10.1038/s41467-025-61017-4.

Correspondence and requests for materials should be addressed to Daixi Li, Wenying Ai or Tao Shen.

Peer review information *Nature Communications* thanks Weisi Guo, Alastair Lennox, who co-reviewed with Mohamed Elsherbini, and the other anonymous reviewer(s) for their contribution to the peer review of this work. A peer review file is available.

Reprints and permissions information is available at http://www.nature.com/reprints

Publisher's note Springer Nature remains neutral with regard to jurisdictional claims in published maps and institutional affiliations.